

## Research Article

# Online Gain-Phase Self-Calibration Method of MIMO Array Based on Statistical Characteristics of Target Angle Distribution

Linwei Wang <sup>1</sup>, Bo Li <sup>1</sup>, Quanrui Zhao <sup>2</sup>, Xiaowei Ji <sup>3</sup>, and Changjun Yu <sup>1</sup>

<sup>1</sup>School of Information Science and Engineering, Harbin Institute of Technology at Weihai, Weihai 264209, China

<sup>2</sup>The 5th Research Department, Shanghai Radio Equipment Research Institute, Shanghai 201109, China

<sup>3</sup>School of Electronics and Information Engineering, Harbin Institute of Technology, Harbin 150001, China

Correspondence should be addressed to Changjun Yu; [yuchangjun@hit.edu.cn](mailto:yuchangjun@hit.edu.cn)

Received 29 May 2022; Accepted 1 July 2022; Published 25 July 2022

Academic Editor: Liu Mingqian

Copyright © 2022 Linwei Wang et al. This is an open access article distributed under the Creative Commons Attribution License, which permits unrestricted use, distribution, and reproduction in any medium, provided the original work is properly cited.

As a hot research topic, the gain-phase error self-calibration in MIMO radar systems has been investigated for many years. In this paper, we proposed a novel array error self-calibration method, termed online errors self-calibration based on feature learning (OES-FL). This method regards the statistical characteristics of the detected targets' DOA as a prior knowledge and does not require the calibrated antenna subarray or external reference source to correct the array disturbances in real time. First, we analyse the monostatic MIMO signal model suffering gain-phase error. Then, we exploit the statistical characteristics of DOA of many targets for correcting gain-phase error of antenna array. Next, the gain-phase error estimation scheme based on LMS and the DOA deviation estimation method based on LSTM are proposed, respectively. Using real-life radar data collected at the integrated transportation hubs to generate simulation data, the proposed approach is shown to be effective in correcting gain-phase errors and, therefore, provides a promising model for online error self-calibration in monostatic MIMO radars.

## 1. Introduction

Direction-of-arrival (DOA) estimation has played an important role in array signal processing over the past few decades [1, 2]. Multiple-input multiple-output (MIMO) technology is first widely used in the field of communication [3–5] and is later introduced into the radar field [6–9]. MIMO radar has gained extensive interest owing to the capability of space diversity [6]. Many DOA estimation algorithms [10–14] have been proposed. Due to the production process, external environment factors, there is always inconsistency among the antenna array elements in practice. The accuracy of DOA estimation is constricted by this inevitable inconsistency [15–17]. As for MIMO radar, the errors of transmit and receive antennas are coupled with each other, thus significantly causes the performance degradation of DOA estimation [18]. Consequently, it is necessary to correct the errors of array, including mutual coupling error, position error, and gain-phase error. In this paper, we focus on developing the approach to mitigate the gain-phase error of MIMO radar array.

Due to the fact that the MIMO radar can generate virtual arrays, the array aperture is enlarged and the number of array elements is increased. Hence, the parameter estimation performance of MIMO radar system is superior than that of conventional phased array radar [7]. Many calibration approaches have been proposed in the literature, an estimating signal parameters via rotational invariance techniques (ESPRIT-) like algorithm has been proposed by Guo et al. [18], which can provide closed-form solution for joint DOD and DOA estimation. Recently, Li et al. [19] proposed an eigenspace based algorithm for joint parameter estimation. This method initially uses the eigenvalue decomposition (EVD) of covariance matrix to acquire the coarse estimation results of DOA and then applies an improved multiple signal classification- (MUSIC-) based cost function to obtain more accurate estimation of DOA. The accurate estimated DOAs interfering with the noise subspace, the error vector of array gain-phase is achieved. Wen et al. [20] proposed a novel parallel factor (PARAFAC) estimator for estimating the DOD and DOA, and this method utilizes the combination of one-dimensional grid searching and least

squares (LS) fitting, which avoids the most of the costly computations generated by eigen decomposition or high-dimension spectrum searching. Li et al. [21] proposed a calibration method for coprime MIMO radar, this method estimates the gain-phase errors by trilinear decomposition, iteratively updated based on least squares, and has an ideal performance. Hu et al. [22] proposed an efficient compressed sensing based DOA method for bistatic MIMO radar with unknown gain-phase errors, which has a high computational efficiency and stability.

These recently proposed methods usually assume that several antennas in the array have been corrected or employ the auxiliary array as a reference. At times associated with complexity of scenario, these corrected antennas or auxiliary array cannot realize. Furthermore, correcting a limited number of antennas also increases the experiment cost, and the antenna array with large scale integration cannot be readily dismantled. Such a kind of self-calibration method would be unsuitable in many field experiments. Consequently, developing a self-calibration approach without any calibrated antennas is very necessary for MIMO radar system. It is the purpose of the present paper to develop a real-time self-calibration approach that accurately estimates the DOA of targets by learning the information acquired by itself.

With the development of machine learning, adaptive technology has made great progress in communication [22–24] and recognition [25, 26]. Real-time parameter optimization can be realized online in a large number of scenarios according to the environment. These experiment conditions in this paper based on a radar system are deployed for a very long period. Although the active calibrated has been carried out, the antenna array must be corroded and damaged after a long time of work, resulting in gain-phase error. Under this common phenomenon, we design an online gain-phase error self-calibration method by considering DOA statistical characteristics of the detected targets as a prior information. We design the gain-phase error estimation method based on LSM and the DOA offset estimation method based on LSTM, which realizes the real-time online error correction achieved without reference sources.

This paper is organized as follows. Section 2 presents a brief description of signal model with gain and phase errors in monostatic MIMO radar. Section 3 focuses on the concepts of the proposed calibration method and its way to achieve. In Section 4, we analyse the performance of the proposed approach using abundant real-life millimeter-wave radar data collected at the junction urban and suburb. Concluding remarks are given in Section 5.

## 2. Signal Model

Theoretical analysis and simulation results are exhibited for illustrating the superiority of the proposed scheme, including the ideal estimation accuracy and the robustness for correcting gain-phase errors. Assume that there is a monostatic MIMO radar system composed of the  $M$  transmit antenna elements and  $N$  receive antenna elements, and  $\mathbf{A}_T(\theta)$  and

$\mathbf{A}_R(\theta)$ , respectively, represent the receive and transmit steering vectors without array gain-phase errors, respectively.

$$\begin{aligned}\mathbf{A}_T(\theta) &= [1 \quad e^{j2\pi d_T \sin(\theta)/\lambda} \quad \dots \quad e^{j2\pi(M-1)d_T \sin(\theta)/\lambda}], \\ \mathbf{A}_R(\theta) &= [1 \quad e^{j2\pi d_R \sin(\theta)/\lambda} \quad \dots \quad e^{j2\pi(N-1)d_R \sin(\theta)/\lambda}],\end{aligned}\quad (1)$$

where  $\theta$  is the DOA of a target, the separation distance between the transmit antenna elements is  $d_T$ , and the  $d_R$  represents separation distance between the receive antenna elements.  $\lambda$  is the wavelength. Suppose that the error of each cell with respect to the first cell is

$$\begin{aligned}\mathbf{\Gamma}_T &= [a_1^T e^{j\phi_1^T} \quad a_2^T e^{j\phi_2^T} \quad \dots \quad a_M^T e^{j\phi_M^T}], \\ \mathbf{\Gamma}_R &= [a_1^R e^{j\phi_1^R} \quad a_2^R e^{j\phi_2^R} \quad \dots \quad a_N^R e^{j\phi_N^R}],\end{aligned}\quad (2)$$

where  $a_m^T$  represents the gain error of the  $m$ th transmit antenna element and  $\phi_m^T$  represents the phase error of the  $m$ th transmit antenna element. Accordingly, the  $a_n^R$  and  $\phi_n^R$  represent the gain error and phase error for  $n$ th receive antenna element, respectively. And particularly,  $a_1 e^{j\phi_1^T} = b_1 e^{j\phi_1^R} = 1$ . Then, the echo signal of the target can be expressed as

$$\mathbf{x}(\theta) = (\mathbf{\Gamma}_T \odot \mathbf{A}_T(\theta)) \otimes (\mathbf{A}_R(\theta) \odot \mathbf{\Gamma}_R), \quad (3)$$

where  $\odot$  represents the Hadamard product, and  $\otimes$  represents the Kronecker product.  $\mathbf{x}(\theta)$  is a vector with a length of  $MN$ , and it can also be reshaped into a  $M \times N$  dimensional matrix  $\mathbf{X}(\theta)$ . In the matrix  $\mathbf{X}(\theta)$ , the element  $x(m, n)$  in  $m$ th row and  $n$ th column represents the echo signal transmitted from the  $m$ th transmit antenna, then reflected from the target and received by the  $n$ th receive antenna element. Hence,  $x(m, n)$  can be expressed as

$$\begin{aligned}x(m, n) &= a_m^T e^{j\phi_m^T} e^{j2\pi(m-1)d_T \sin(\theta)/\lambda} e^{j2\pi(n-1)d_R \sin(\theta)/\lambda} a_n^R e^{j\phi_n^R} \\ &= a_m^T a_n^R e^{j(2\pi(m-1)d_T \sin(\theta)/\lambda + 2\pi(n-1)d_R \sin(\theta)/\lambda + \phi_m^T + \phi_n^R)}.\end{aligned}\quad (4)$$

When separating the amplitude and the phase, we can obtain

$$\begin{aligned}A(m, n) &= a_m^T a_n^R, \\ \Phi(m, n) &= K(m, n) \sin(\theta) + \phi_m^T + \phi_n^R,\end{aligned}\quad (5)$$

where  $K(m, n) = [2\pi(m-1)d_T + 2\pi(n-1)d_R]/\lambda$  and the amplitude error can be obtained according to the previous  $A(m, n)$ . As for obtaining phase error,  $\phi_1^T$  and  $\phi_1^R$  are known, and the rest part of the antenna errors can be solved by the following equation.

$$\Phi = \mathbf{H}\mathbf{X}, \quad (6)$$

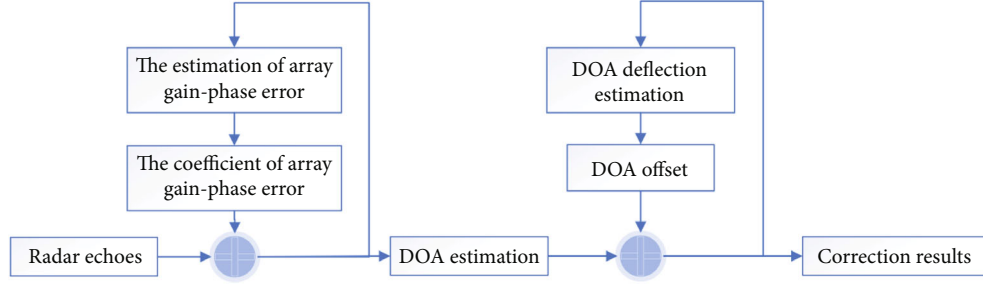


FIGURE 1: Flowchart diagram of proposed algorithm.

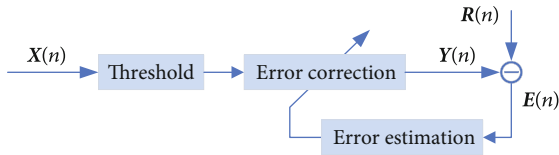


FIGURE 2: LMS algorithm processing scheme.

where  $\Phi = [\Phi(1, 2) \quad \Phi(1, 3) \quad \cdots \quad \Phi(1, N) \quad \Phi(2, 1) \quad \cdots \quad \Phi(M, N)]$ ,

$$\mathbf{H} = \begin{bmatrix} & & & 1 & & & & & & K(1,2) \\ & & & & \ddots & & & & & \vdots \\ & & & & & & & & 1 & K(1,N) \\ 1 & & & & & & & & & K(2,1) \\ 1 & & & & & & 1 & & & K(2,2) \\ \vdots & & & & & \ddots & & & & \vdots \\ 1 & & & & & & & & 1 & K(2,N) \\ 1 & & & & & & & & & K(3,1) \\ 1 & & & & & & 1 & & & K(3,2) \\ \vdots & & & & & \ddots & & & & \vdots \\ 1 & & & & & & & & 1 & K(3,N) \\ & & \ddots & & & & & & & \vdots \\ & & & 1 & & & & & 1 & K(M,N) \end{bmatrix},$$

$$\mathbf{X} = [\phi_2^T \quad \phi_3^T \quad \cdots \quad \phi_M^T \quad \phi_2^R \quad \phi_3^R \quad \cdots \quad \phi_N^R \quad \sin \theta].$$

Equation (6) can be viewed as an equation set of multiple variables consisting of  $MN - 1$  linear equations. Because the last column of  $\mathbf{H}$  can be represented by a linear combination of the previous  $M + N$  columns, the maximum rank of this matrix is  $M + N - 2$ . And the total number of unknowns is  $M + N - 1$ ; obviously, this equation has multiple solutions, and the additional information is required to determine the value of each unknown. In the active calibration technology, where  $\theta$  is known, that full rank can be satisfied, and the errors of each element can be solved. For the self-calibration algorithm,  $\theta$  is unknown, as long as the error of any element is known, that is to say, one antenna is calibrated in this array, and the phase errors of each element can be obtained.

### 3. Error Calibration Method

**3.1. Theoretical Model.** The previous methods usually estimate the DOA of the targets by applying the calibrated antennas and then estimate the gain-phase errors of other elements in the array according to the DOA of targets. If

the gain-phase errors of all antenna elements are unknown, Equation (6) has infinite number of solutions. In addition, if a phase error between two elements in array is ignored, a wrong DOA estimation result will be obtained by this pair of elements. When utilizing this wrong DOA estimation result to further estimate the error of other antenna elements, all the results are a function of the element that we ignored. And the DOA results of this array will also have a fixed phase deviation, which is the phase error of the ignored element. Using this correction result to estimate the DOA of targets again, all the obtained results will have a fixed deviation. In this scenario, when the distribution characteristics of targets' DOA are identified, the errors of DOA will be corrected. Therefore, we propose a calibration algorithm model as shown in Figure 1. The calibration algorithm model consists of two parts: error estimation and DOA deflection estimation.

In the error estimation, we first ignore the error of an antenna element, and anyone has opportunity to be tentatively ignored. For example, we ignore the error of the second transmit antenna element,  $\hat{\phi}_2^T = 0$ , hence, the Equation (6) has only one unique solution as follows.

$$\begin{aligned} \hat{\phi}_m^T &= \Phi(m, 1) - (m - 1)\Phi(2, 1), \\ \hat{\phi}_n^R &= \Phi(1, n) - (n - 1)\Phi(2, 1) \frac{d_R}{d_T}. \end{aligned} \quad (7)$$

As for another target with direction  $\varphi$ , the array echo calibrated by Equation (7) is as follows.

$$\begin{aligned} \Phi_\varphi(m, n) &= K(m, n) \sin(\varphi) + \phi_m^T - \hat{\phi}_m^T + \phi_n^R - \hat{\phi}_n^R \\ &= K(m, n) \sin(\varphi) + \left[ (m - 1) + (n - 1) \frac{d_R}{d_T} \right] \phi_2^T \\ &= K(m, n) \left[ \sin(\varphi) + \frac{\lambda \phi_2^T}{2\pi d_T} \right]. \end{aligned} \quad (8)$$

In practice, there is a fixed phase offset  $\Delta\varphi = \lambda \phi_2^T / (2\pi d_T)$  when the DOA of target is estimated after correcting. If the distribution of real targets obeys a normal distribution and the mean of DOAs is  $0^\circ$ , the results will have a fixed deviation after the calibration. The mean is changed as  $\arcsin(\Delta\varphi)$ . The mean of DOAs can be obtained by applying a great

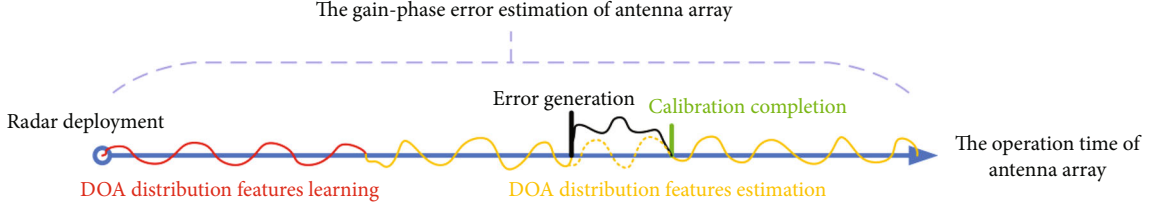


FIGURE 3: Proposed approach description and main steps.

deal of statistical information, so  $\Delta\varphi$  can be estimated, and the accurate calibration is realized.

**3.2. Algorithm Flow.** Assume that targets with different distances and speeds have been separated by applying coherent integration and eigenvalue decomposition in the signal processing process, thus, the echo  $\mathbf{X}(\theta)$  only contains one target. In order to weaken the interference of noise, least mean square (LMS) is used to iteratively calculate the gain-phase error of array, and the target with high SNR is selected for estimating gain-phase errors during each iteration.

Figure 2 illustrates the processing scheme of LMS, where the  $\mathbf{X}(n)$  represents the  $n$ th echo data. The targets with high SNR are selected, which can grant the ideal accuracy and efficiency of estimation, and these selected targets are put into the successive iteration for estimating the gain-phase errors.  $\mathbf{Y}(n)$  represents the corrected results of output, and  $\mathbf{R}(n)$  as the reference signal is the theoretical echo data corresponding to the estimated DOA by using the first two elements in  $\mathbf{X}(n)$ ,  $x_1(n)$  and  $x_2(n)$ . The estimated DOA  $\hat{\theta}$  can be defined as

$$\hat{\theta} = \arcsin \left\{ \text{angle} \left[ \frac{x_2(n)}{x_1(n)K(1,2)} \right] \right\}. \quad (9)$$

Hence, the reference signal is defined as

$$\mathbf{R}(n) = \begin{bmatrix} 1 & e^{jK(1,2) \sin(\hat{\theta})} & \dots & e^{jK(M,N) \sin(\hat{\theta})} \end{bmatrix}. \quad (10)$$

The equation for the  $\mathbf{Y}(n)$  and  $\mathbf{E}(n)$  can be described as

$$\begin{aligned} \mathbf{Y}(n) &= \mathbf{X}(n)\mathbf{W}(n), \\ \mathbf{E}(n) &= \mathbf{R}(n) - \mathbf{Y}(n), \\ \mathbf{W}(n+1) &= \mathbf{W}(n) + \alpha\mathbf{E}(n)\mathbf{X}^*(n), \end{aligned} \quad (11)$$

where  $\mathbf{W}(n)$  is the calibrated coefficient,  $\alpha$  represents the learning factor, and  $\mathbf{X}^*(n)$  is the conjugate for  $\mathbf{X}(n)$ . After completing the iteration, we obtain  $\mathbf{W} \in \mathbb{C}^{MN \times 1}$  which is the calibration coefficient of the virtual array, and  $\mathbf{W}$  could be reshaped into a matrix  $\bar{\mathbf{W}} \in \mathbb{C}^{M \times N}$ . The ratio of each column of  $\bar{\mathbf{W}}$  to the other is the error between the two transmit elements; similarly, the ratio of each row of  $\bar{\mathbf{W}}$  to the other is the error between the two receive elements. We can get the gain-phase errors of transmit array  $\hat{\Gamma}_T$  and that of receive

array  $\hat{\Gamma}_R$  as follows.

$$\begin{aligned} \hat{\Gamma}_T &= \frac{\bar{\mathbf{W}}\bar{\mathbf{W}}^\dagger}{N}, \\ \hat{\Gamma}_R &= \frac{(\bar{\mathbf{W}}_R^\dagger \bar{\mathbf{W}})^T}{M}, \end{aligned} \quad (12)$$

where  $\bar{\mathbf{W}}_C \in \mathbb{C}^{1 \times N}$  is the first column of  $\bar{\mathbf{W}}$ ,  $\bar{\mathbf{W}}_R \in \mathbb{C}^{M \times 1}$  is the first row of  $\bar{\mathbf{W}}$ , and  $(\cdot)^\dagger$  is the pseudoinverse of a matrix.

Then, the DOA offset is estimated by using the statistical characteristics of the targets' DOA. In most cases, when deploying a new antenna array, all the antenna elements should be calibrated and tested. Consequently, there is a reasonable prospect that the intrinsic error of antenna array has been calibrated, and then, radar can normally operate over an ideal period. While a considerable amount of work has been done, the antenna array system absolutely be damaged due to the corrosion and wear of antennas, which causes the gain-phase errors of the antennas. We can use the detection data of the radar system recently deployed radar system to collect the characteristics of the DOA distribution of targets, and then, these characteristics will as reference data to correct the errors generated in the subsequent work.

For radars used to detect fixed areas or basically unchanged scenes, the statistical characteristics of the DOA of detected target are relatively stable in a long observation period. It is not surprised that the fluctuations of DOA characteristics in a short term also can be found.

Such as the road surveillance radar, it is used to monitor a confined area. For an urban highway, a large number of people leave from the residential area to the workplace in the morning, and the number of vehicles leaving the residential area will be significantly more than the vehicles entering the residential area, so that the average DOA of targets in a short period tends toward the side of the lane leaving the residential area. In contrast, when people return to the residential area in the evening, the average DOA of targets will tend toward the other side. In this paper, the DOA distribution characteristics of targets are estimated by using LSTM network. Together, the learning of DOA distribution characteristics in the initial stage helps to readily predict the distribution characteristics in the following stage, which ensures to timely calibrate the antennas array. There have been aroused interests in the performance capabilities of DOA estimation. Figure 3 shows the description above.



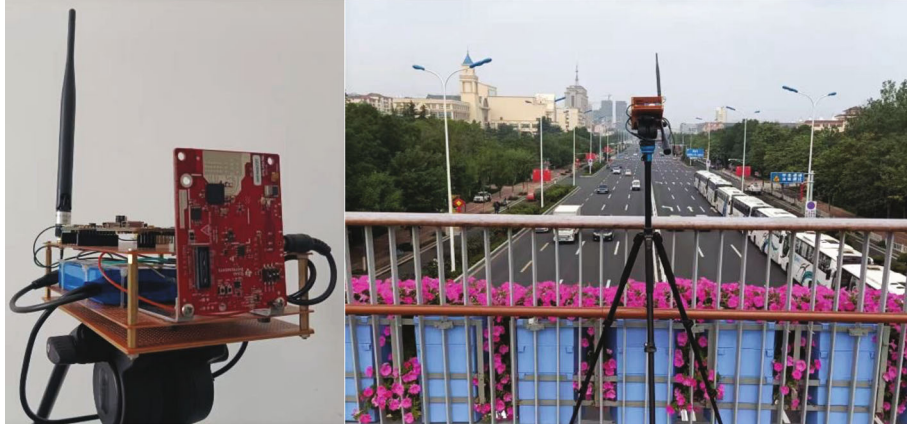


FIGURE 4: Images of millimeter-wave radar in the field experiment.

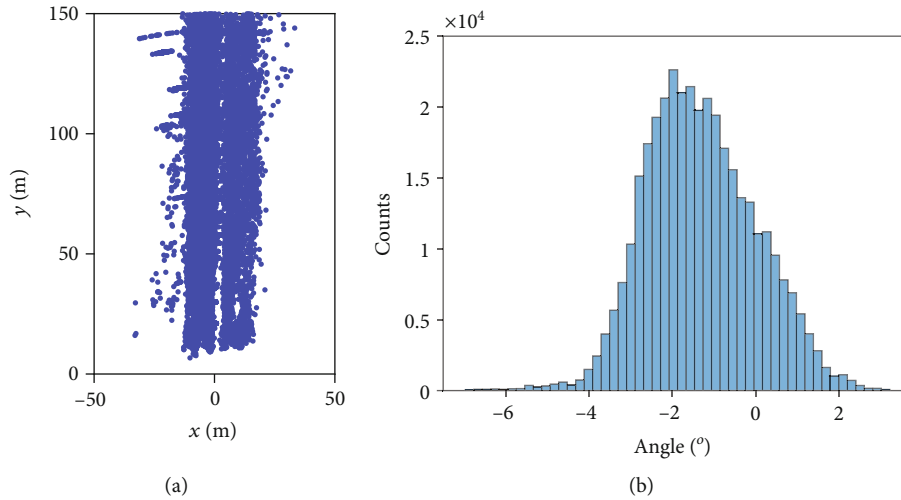


FIGURE 5: Targets detection results. (a) The location map of 354,000 targets. (b) The histogram of DOA distribution of 354,000 targets.

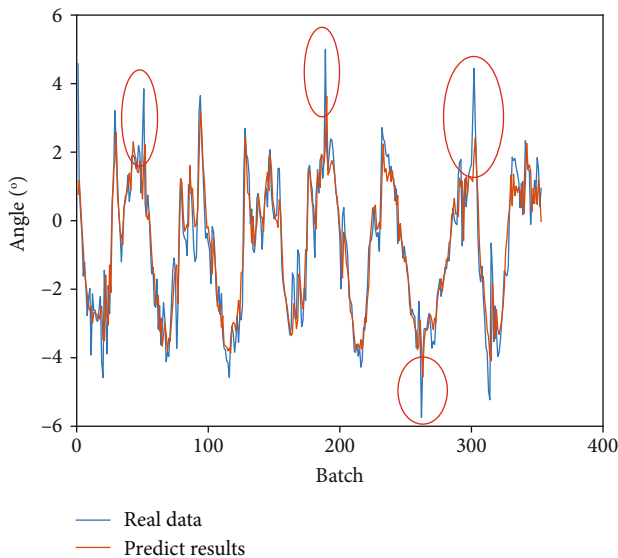


FIGURE 6: The prediction results of the DOA mean value of each group by using LSTM network.

### 4. Experiment Results and Discussion

We conducted an experiment with a millimeter-wave radar to monitor vehicles on the road. The radar is deployed on the pedestrian bridge where the main road connects the suburb and the urban area. A typical road monitoring installation along the middle of the road is shown in Figure 4.

We collected 14440 batches of data, containing a total of 354,000 targets. The distribution of the captured samples points is shown in Figure 5(a). And the histogram of DOA distribution is shown in Figure 5(b).

We first count the DOA of the targets in each frame of data, and all the average DOA of these targets was about -2 degrees. Then, we divide the 354,000 targets into 354 groups, and each group consists of 1000 detected targets. Next, the mean value of DOA of each group is calculated. Finally, the LSTM network is applied to estimate the mean value of the targets' DOA. The applied LSTM has 128 hidden units, the first 300 groups data are applied for training, and the rest of the groups are used for testing the prediction performance of LSTM. The prediction results are shown in Figure 6. As shown in Figure 6, the blue curve represents

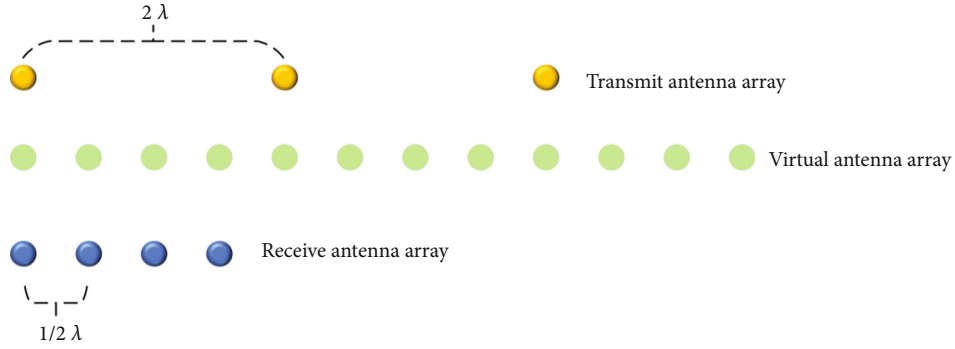


FIGURE 7: Schematic diagram of antenna array structure.

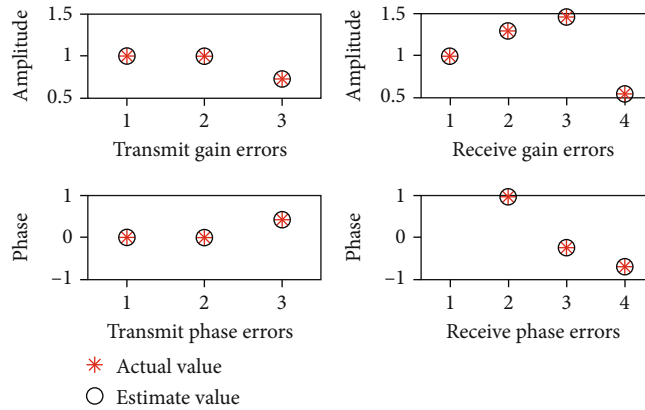


FIGURE 8: Gain-phase errors estimate results with SNR=30dB.

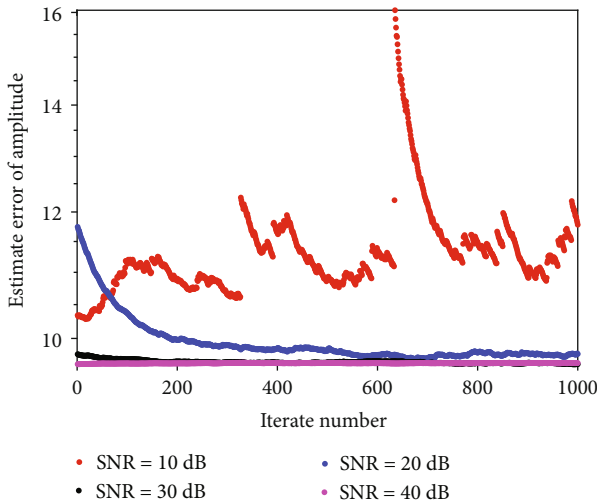


FIGURE 9: Estimate error of gain in different SNR.

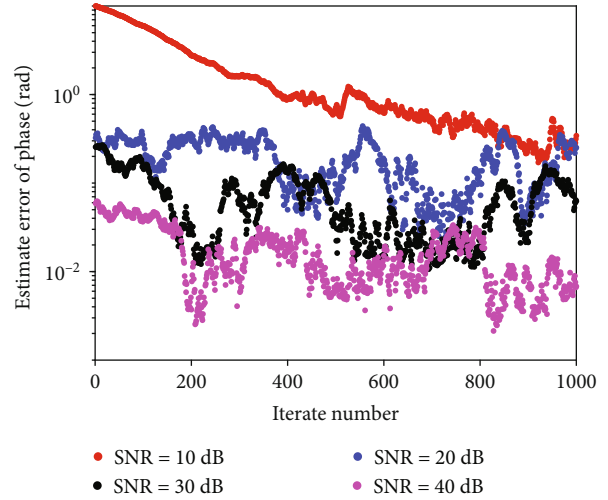


FIGURE 10: Estimate error of phase in different SNR.

the real DOA of 354 groups, and the red curve represents the predicted DOA by using LSTM network. Generally, the predicted results curve approaches to the real DOA. But we also find that some spikes and highlight them by using red circles. This phenomenon can be attributed that the amount of the data is not sufficient for training more ideal network

structure, and we will also further improve the design of the LSTM network in the next work.

In order to verify the gain-phase error estimation ability of LMS algorithm, a set of original data are generated according to the detected target information. Specifically, suppose that a radar has three transmitting antennas and four receiving antennas, as depicted in Figure 7 where the

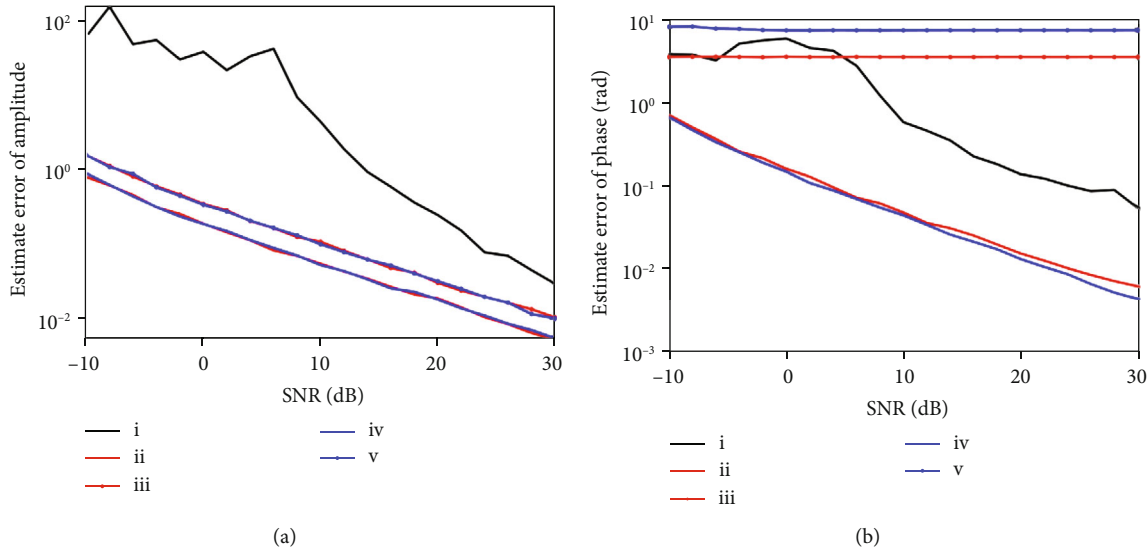


FIGURE 11: Estimate error compared with previous study. (a) The gain estimate error in different SNR. (b) The phase estimate error in different SNR. (i) are the results of LMS, (ii) are the results of MUSIC with 5 calibrated elements, (iii) are the results of MUSIC with 2 calibrated elements, (iv) are the results of ESPRIT with 5 calibrated elements, and (v) are the results of ESPRIT with 2 calibrated elements.

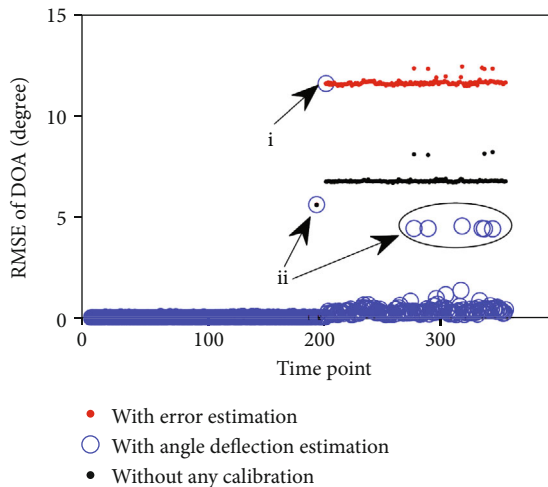


FIGURE 12: RMSE of DOA with a close to reality scenario, the gain-phase errors appear at (i), and (ii) is affected by SNR.

space between receiving antennas is half wavelength, the space between transmitting antennas is two times wavelength, and a 12-element virtual uniform linear array can be obtained. The simulated echo data is generated by associating with the information of detected real target, and the DOA of simulated data is the same as real data.

We used LMS algorithm to calibrate the gain-phase errors, and the estimated errors are shown in Figure 8. We assume that transmitting antenna 1, 2, and receiving antenna 1 have no errors, and other antennas have random gain-phase errors. The gain errors are uniformly distributed between 0.5 and 1.5, and the phase errors are uniformly distributed between  $-\pi/2$  and  $\pi/2$ . The SNR of targets are 30 dB. The red stars represent the real gain or phase errors, and the black circle represents the estimated results. Clearly,

the result comparison of estimated and real data implies that the proposed method successfully estimates the unknown targets.

Furthermore, for assessing the SNR effect for estimation accuracy, the simulations are run by performing different SNRs iterates from 0 to 1000. Figures 9 and 10 show the exemplary of the distinct relationship between the SNR and estimation accuracy, the SNR is higher, and the estimation accuracy is more ideal. This results also imply that the value of SNR has a considerable effect on estimation accuracy, so selecting the data with high SNR as input data can sufficiently facilitate the estimation performance of LMS.

Figure 11 shows the estimate error results of different algorithm. The simulation of LMS is conducted with 1000 iterates. A target with random angle is generated in each iterate. The simulation of MUSIC and ESPRIT is conducted with a target with 1000 snapshots. There are 2 experiments for MUSIC and ESPRIT, respectively. There are 2 elements that have been calibrated well in one experiment and 5 calibrated well elements in another. The results are the mean of 200 Monte Carlo trials for every experiments. Although the performance of LMS for gain error estimation is lower than others, but has a stable phase error estimation performance with only 2 elements.

At last, we simulate a real-world problematic situation, a MIMO radar system is deployed with well down calibration, and the stochastic gain-phase errors appear in every antenna element after a period of time. We simulated the process of such a scenario to verify the proposed method. The gain-phase errors appear in the 201th time point. Figure 12 shows the RMSE of DOA estimation of 1000 targets changed over time.

Figure 12 describes the RMSE of DOA, and we can observe that the value of RMSE is small in the absence of errors. At the i point, the estimation performance of DOA

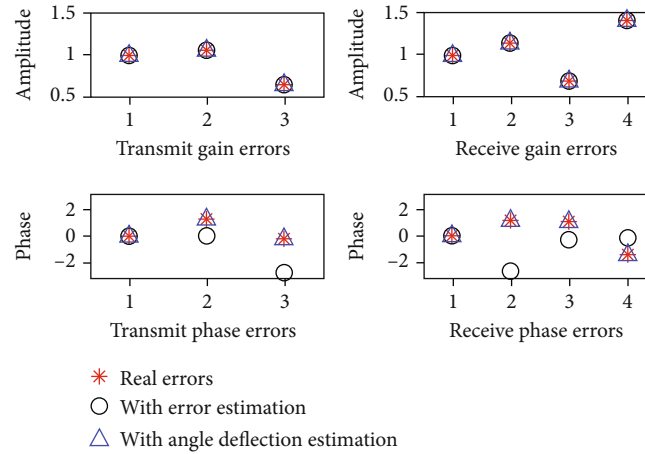


FIGURE 13: The phase error estimation results.

is suddenly degraded, which is depicted in black dots. After correcting the gain-phase error, the estimation performance of DOA is worse than before. However, after correcting DOA offset, the value of RMSE is obviously lower than before, which is shown in blue circle. At the ii point, some points appear in Figure 12, which can be attribute that the SNR of target is generated according to the SNR of real data, and the SNR at some moments is relatively small, causing a larger RMSE. But this phenomena does not affect the overall conclusion.

The results of phase error are shown in Figure 13. The amplitude errors can be estimated well with the error estimation by LMS, while the phase errors still have a deflection, which can be accurately estimated after angle deflection estimation using LSTM.

## 5. Conclusions

In this paper, an online calibration method of array gain-phase error has been proposed for a variety of radar array. This online error calibration method considering the characteristic of DOA distribution applies LSTM network to predict the subsequent DOA. The proposed method is feasible and simply operated because it does not require the external reference source or some calibrated antenna. Hence, the proposed method can be readily applied to long-term range surveillance of various targets due to the cost-effective advantage and feasible establishment. Numerical examples demonstrate improvements in high resolution multiple source locations, which has confirmed that taking the DOA distribution characteristic of targets as priori information and sufficiently learning this information can address problem concerning DOA estimation. Despite the promising results, this analysis opens new research directions, all aimed to improve the proposed algorithm system adaptability and confidence in enhancing estimation accuracy.

## Data Availability

The data used to support the findings of this study are available from the corresponding author upon request.

## Conflicts of Interest

The authors declare that there is no conflict of interest regarding the publication of this paper.

## Acknowledgments

The research and publication of the article were funded by the National Natural Science Foundation of China (no. 62031015, no. 62171154, and no. 61971156), the Natural Science Foundation of Shandong Province (no. ZR2020MF007 and no. ZR2020MF013), and the Research Fund Program of Guangdong Key Laboratory of Aerospace Communication and Networking Technology (no. 2018B030322004).

## References

- [1] H. Krim and M. Viberg, "Two decades of array signal processing research: the parametric approach," *IEEE Signal Processing Magazine*, vol. 13, no. 4, pp. 67–94, 1996.
- [2] H. L. Trees Van, "Appendix B: array processing literature," in *Detection, Estimation, and Modulation Theory, Optimum Array Processing*, pp. 1407–1413, John Wiley & Sons, 2002.
- [3] A. B. Gershman and N. D. Sidiropoulos, "Space-time processing for MIMO communications," 2005, May 28, 2022, [https://xueshu.baidu.com/usercenter/paper/show?paperid=d4cf071f317caec1dffdf34fa6626ed&site=xueshu\\_se](https://xueshu.baidu.com/usercenter/paper/show?paperid=d4cf071f317caec1dffdf34fa6626ed&site=xueshu_se).
- [4] E. G. Larsson, O. Edfors, F. Tufvesson, and T. L. Marzetta, "Massive MIMO for next generation wireless systems," *IEEE Communications Magazine*, vol. 52, no. 2, pp. 186–195, 2014.
- [5] Y. Xu, B. Li, N. Zhao et al., "Coordinated direct and relay transmission with NOMA and network coding in Nakagami-m fading channels," *IEEE Transactions on Communications*, vol. 69, no. 1, pp. 207–222, 2021.
- [6] E. Fishler, A. Haimovich, R. Blum, D. Chizhik, L. Cimini, and R. Valenzuela, "MIMO radar: an idea whose time has come," in *Proceedings of the 2004 IEEE Radar Conference (IEEE Cat. No.04CH37509)*, pp. 71–78, Philadelphia, PA, USA, 2004.
- [7] E. Fishler, A. Haimovich, R. Blum, R. Cimini, D. Chizhik, and R. Valenzuela, "Performance of MIMO radar systems: advantages of angular diversity," in *Conference Record of the Thirty-*



- Eighth Asilomar Conference on Signals, Systems and Computers, 2004*, pp. 305–309, Pacific Grove, CA, USA, 2004.
- [8] D. W. Bliss, K. W. Forsythe, S. K. Davis et al., “GMTI MIMO radar,” in *2009 International Waveform Diversity and Design Conference*, pp. 118–122, Kissimmee, FL, USA, 2009.
- [9] M. Liu, B. Li, Y. Chen et al., “Location parameter estimation of moving aerial target in space–air–ground-integrated networks-based IoV,” *IEEE Internet of Things Journal*, vol. 9, no. 8, pp. 5696–5707, 2022.
- [10] X. Zhang, L. Xu, L. Xu, and D. Xu, “Direction of departure (DOD) and direction of arrival (DOA) estimation in MIMO radar with reduced-dimension MUSIC,” *IEEE Communications Letters*, vol. 14, no. 12, pp. 1161–1163, 2010.
- [11] M. L. Bencheikh and Y. Wang, “Joint DOD-DOA estimation using combined ESPRIT-MUSIC approach in MIMO radar,” *Electronics Letters*, vol. 46, no. 15, pp. 1081–1083, 2010.
- [12] F. Wen, Z. Zhang, and G. Zhang, “Joint DOD and DOA estimation for bistatic MIMO radar: a covariance trilinear decomposition perspective,” *IEEE Access*, vol. 7, pp. 53273–53283, 2019.
- [13] A. M. Ahmed, U. S. K. P. M. Thanthrige, A. E. Gamal, and A. Sezgin, “Deep learning for DOA estimation in MIMO radar systems via emulation of large antenna arrays,” *IEEE Communications Letters*, vol. 25, no. 5, pp. 1559–1563, 2021.
- [14] X. Hua, Y. Ono, L. Peng, Y. Cheng, and H. Wang, “Target detection within nonhomogeneous clutter via total Bregman divergence-based matrix information geometry detectors,” *IEEE Transactions on Signal Processing*, vol. 69, pp. 4326–4340, 2021.
- [15] H. Srinath and V. U. Reddy, “Analysis of MUSIC algorithm with sensor gain and phase perturbations,” *Signal Processing*, vol. 23, no. 3, pp. 245–256, 1991.
- [16] H. Li, J. Geng, and J. Xie, “Robust adaptive beamforming based on covariance matrix reconstruction with RCB principle,” *Digital Signal Processing*, vol. 127, article 103565, 2022.
- [17] M. Liu, Z. Liu, W. Lu, Y. Chen, X. Gao, and N. Zhao, “Distributed few-shot learning for intelligent recognition of communication jamming,” *IEEE Journal of Selected Topics in Signal Processing*, vol. 16, no. 3, pp. 395–405, 2022.
- [18] Y. D. Guo, Y. S. Zhang, and N. N. Tong, “ESPRIT-like angle estimation for bistatic MIMO radar with gain and phase uncertainties,” *Electronics Letters*, vol. 47, no. 17, pp. 996–997, 2011.
- [19] L. Li, T. Fu, Y. Yang, M. Huang, Z. Han, and J. Li, “Joint angle estimation and array calibration using eigenspace in monostatic MIMO radar,” *IEEE Access*, vol. 8, pp. 60645–60652, 2020.
- [20] F. Wen, J. Shi, X. Wang, and L. Wang, “Angle estimation for MIMO radar in the presence of gain-phase errors with one instrumental Tx/Rx sensor: a theoretical and numerical study,” *Remote Sensing*, vol. 13, no. 15, p. 2964, 2021.
- [21] J. Li, L. He, Y. He, and X. Zhang, “Joint direction of arrival estimation and array calibration for coprime MIMO radar,” *Digital Signal Processing*, vol. 94, pp. 67–74, 2019.
- [22] J. Hu, E. Baidoo, L. Zhan, and Y. Tian, “Computationally efficient compressed sensing-based method via FG Nyström in bistatic MIMO radar with array gain-phase error effect,” *International Journal of Antennas and Propagation*, vol. 2020, Article ID 1586353, 12 pages, 2020.
- [23] W. Lu, P. Si, G. Huang et al., “SWIPT cooperative spectrum sharing for 6G-enabled cognitive IoT network,” *IEEE Internet of Things Journal*, vol. 8, no. 20, pp. 15070–15080, 2021.
- [24] Y. Xu, J. Tang, B. Li, N. Zhao, D. Niyato, and K.-K. Wong, “Adaptive aggregate transmission for device-to-multi-device aided cooperative NOMA networks,” *IEEE Journal on Selected Areas in Communications*, vol. 40, no. 4, pp. 1355–1370, 2022.
- [25] W. Lu, Y. Ding, Y. Gao et al., “Resource and trajectory optimization for secure communications in dual unmanned aerial vehicle mobile edge computing systems,” *IEEE Transactions on Industrial Informatics*, vol. 18, no. 4, pp. 2704–2713, 2022.
- [26] M. Liu, C. Liu, M. Li, Y. Chen, S. Zheng, and N. Zhao, “Intelligent passive detection of aerial target in space-air-ground integrated networks,” *China Communications*, vol. 19, no. 1, pp. 52–63, 2022.